

Abstract

We develop a double mean-field theory for charged macrogels immersed in electrolyte solutions in the spirit of the cell model approach. We first demonstrate that the equilibrium sampling of a single explicit coarse-grained charged polymer in a cell yields accurate predictions of the swelling equilibrium if the geometry is suitably chosen and all pressure contributions have been incorporated accurately. We then replace the explicit flexible chain by a suitably modeled penetrable charged rod that allows to compute all pressure terms within the Poisson-Boltzmann approximation. This model, albeit computationally cheap, yields excellent predictions of swelling equilibria under varying chain length, polymer charge fraction, and external reservoir salt concentrations when compared to coarse-grained molecular dynamics simulations of charged macrogels. We present an extension of the model to the experimentally relevant cases of pH-sensitive gels.

Modeling gel swelling equilibrium in mean-field: From explicit models to Poisson-Boltzmann

Jonas Landsgesell* David Sean Patrick Kreissl
Kai Szuttor Christian Holm

November 20, 2021

Polyelectrolyte gels consist of crosslinked charged polymers (polyelectrolytes) that can be synthesized with various topologies and are produced in sizes ranging from nanometers (nanogels) up to centimeters (macrogels) [1, 2]. They show a large, reversible uptake of water that is exploited in numerous daily-life products, such as in superabsorbers, cosmetics, pharmaceuticals [3, 4, 5], agriculture [6, 7], or quite recently water desalination [8, 9]. Tailoring polyelectrolyte gels to their applications requires a sufficiently accurate prediction of their swelling capabilities and elastic responses, a task that still goes beyond analytical approaches [10, 11, 12, 13, 14, 15, 16, 17, 18]. So far only all-atom simulations of short single chains in the bulk (not of whole hydrogels) with explicit water have been performed [19, 20, 21, 22]. On the other hand, coarse-grained polyelectrolyte network models have demonstrated their ability to amend analytical approaches, showing that structural microscopic details can have noticeable effects on the macroscopic properties such as the swelling [23, 24, 25, 26, 27, 28, 29, 30, 31, 32]. Macroscopic gels with monodisperse chain length can be simulated with microscopic detail using molecular dynamics (MD) simulations with periodic boundary conditions (PBCs) (cf. *periodic gel model*) where a unit gel section is connected periodically to yield an infinite gel without boundaries. However, even MD simulations of periodic gels remain computationally very expensive due to the many particles and the slow relaxation times of the involved polymers. Thus, the development of computationally efficient mean-field models capable of predicting swelling equilibria have been of scientific interest in the last years [33, 15, 31, 32]. First ideas of using a Poisson-Boltzmann (PB) cell model under tension were put forward by Mann for salt-free gels, with moderate success [33].

About sixty years ago Katchalsky and Michaeli [11] suggested a free energy model that has recently been shown to predict swelling equilibria reasonably well [31] when compared to MD simulations of charged bead-spring gels. This model has been applied to explore a wide parameter space in search of optimal desalination conditions [9]. However, the Katchalsky model fails [31] for Manning parameters $\xi = \lambda_B / \langle d \rangle > 1$ [34], where λ_B denotes the Bjerrum length, and

*Institute for Computational Physics, University of Stuttgart, D-70569 Stuttgart, Germany

$\langle d \rangle$ the average distance between polymer backbone charges. This is presumably due to the usage of the Debye-Hückel approximation.

In this letter we describe two successive mean-field approaches to render the determination of swelling equilibria of polyelectrolytes accurately and efficiently. Figure 1 displays our construction scheme of the two different models. First, we describe a *single-chain MD cell model*, that reproduces results similar to those obtained from expensive MD simulations of multiple crosslinked chains. This reduces the many-body problem of the macroscopic gel to one of computing the pressure exerted within a cell containing a single polyelectrolyte chain under varying environmental conditions. The single-chain cell model can thus be viewed as a mean-field attempt to factorize the many-body partition function of the macrogel into a product state of suitable identical subunits [35]. We then show that the single-chain cell model can further be simplified in a second mean-field step using a PB description of the chain with appropriate boundary conditions. The PB cell description has been successful in describing a variety of polyelectrolyte phenomena [36, 37, 38, 39, 40, 41] and is here applied to macroscopic polyelectrolyte gels for the first time. The quality of our two mean-field models is gauged by comparing them to 60 data points for the swelling equilibrium of periodic monodisperse gel MD simulations obtained within a wide range of system parameters. We want to emphasize that none of our models assumes a specific stretching state of the chains: they are constructed to incorporate the main physical effects which happen during stretching (at high chain extensions) and compression of a polyelectrolyte gel (at low chain extensions).

Finally, we generalize the PB cell model to account for the effect of weak groups along the chain backbone. From this we can efficiently predict swelling equilibria for the experimentally relevant cases of weak polyelectrolyte gels.

We specifically compare our results to MD data for the *periodic gel model* obtained by Košovan et. al [31] where a continuum solvent is used with standard charged bead-spring polymers connected in a diamond lattice as in the work of Ref. [27] together with explicit salt and counterions. Here a perfect tetrafunctional gel is described by the chain length N and the monomers charge fraction f . This explicit particle based model uses monodisperse chain lengths which is in contrast to the heterogeneity observed in a wide variety of synthesized gels [42]. It would be computationally very costly to introduce chain length heterogeneity into this model since it would require to simulate a much larger representative volume element. However, these periodic gel simulations of a monodisperse gel are sufficient to test the validity of our two consecutive mean-field approaches.

All MD simulations (namely the periodic gel and the single-chain model described later) are performed with PBCs using the simulation package ESPResSo [43, 44]. All particles interact via WCA interactions [45, 46]. Monomers are connected via FENE bonds (including the ends of the single periodic chain) with Kremer-Grest parameters [47]. We employ the Langevin thermostat [48], and all electrostatic interactions between particles are calculated with the P3M method [49] tuned to an accuracy in the root mean squared error of the electrostatic force of at least 10^{-3} in electrostatic simulation units [50].

In addition, salt ion pair exchanges between the simulation volume and an external reservoir are performed using grand canonical Monte Carlo moves [48]. The equilibrium pressure inside the gel and the electro-chemical potentials of all i species balance out with that of the reservoir: $P_{\text{in}}(V_{\text{eq}}) = P_{\text{res}}$ and $\mu_i^{\text{gel}} = \mu_i^{\text{res}}$, respectively. The simulations are performed at different imposed volumes and the internal pressure is measured after chemical equilibrium is reached. The reservoir pressure is approximated by the ideal gas expression $P_{\text{res}} = \sum_i k_{\text{B}} T c_i^{\text{b}}$, with the Boltzmann constant k_{B} , temperature T and bulk ion concentrations c_i^{b} , which are chosen such that the bulk is electroneutral.

The above approach requires multiple simulations at different imposed volumes until the condition $P_{\text{in}}(V_{\text{eq}}) = P_{\text{res}}$ can be narrowed down to a satisfactory small interval. The equilibrium volume is found at the intersection of $P_{\text{in}}(V_{\text{eq}})$ and P_{res} by using linear interpolation. The errorbar is given by the width of the interval. Under equilibrium conditions, the end-to-end distance R_{e} is equal to the equilibrium chain extension R_{eq} .

The first model for complexity reduction is the mean-field single-chain model. Like in the cylindrical cell model used to describe solutions of polyelectrolytes [38, 40, 41], we propose constructing the many-body partition function of a periodic gel as a suitable product of individual cylindrical cells containing a single polyelectrolyte chain with added salt. Since the main physical principle is the balance between the polyelectrolyte chain tension and the remaining pressure contributions (mainly the ionic ones), these cylindrical cells have an axial length chosen such as to represent the polymer chain extension between gel crosslinks. Like in the periodic gel model, we perform MD simulations for a single-chain in cylindrical confinement allowing explicit salt ion pairs to enter the cell volume and reach chemical equilibrium with an external reservoir [48]. For a perfect affine compression of a (fully stretched) tetrafunctional gel (built in a diamond cubic lattice) the volume per chain is given by: $V_{\text{chain}} = R_{\text{e}}^3/A$, with the geometrical prefactor $A = \sqrt{27}/4$ [31]. Using the volume of the cylindrical cell as the volume per chain, we arrive at a constant aspect ratio $R_{\text{out}}/R_{\text{e}} = 1/\sqrt{\pi A} \approx 0.49$, where R_{out} denotes the radius of the cylindrical cell, see Fig. 1. This is in contrast to the deformation of a pure isolated chain, which does not occupy a cylindrical volume of constant aspect ratio upon a stretching deformation. The simulation volume is completely defined by the length of the cylinder, or equivalently R_{e} ¹. Note that the single chain under confinement sees its images in the axial direction (due to PBCs) which in a simplified way mimics the electrostatic environment in a gel, where the end of a single chain sees the next chain. For cylindrical geometries under affine compression, the pressure inside the volume is given by [41, 51]:

$$P_{\text{in}} = \frac{1}{3}P_{\text{cap}} + \frac{2}{3}P_{\text{side}}, \quad (1)$$

where the total internal pressure P_{in} is split into the two contributions from, P_{cap} , the cylinder end caps and, P_{side} , the side wall. The latter is mainly

¹In the single chain MD simulations the cylinder height is $R_{\text{e}} + b$ (with the average bond length $b \approx 0.966\sigma$) in order to be able to satisfy PBCs.

dominated by collisions between mobile ions and the boundary whereas the cap pressure is given as the (z, z) component of the pressure tensor $P_{\text{cap}} = \Pi_{(z,z)}$:

$$\Pi_{(z,z)} = \frac{\sum_i m_i v_i^{(z)} v_i^{(z)}}{V} + \frac{\sum_{j>i} \vec{F}_{ij}^{(z)} \cdot \vec{r}_{ij}^{(z)}}{V} + \Pi_{(z,z)}^{\text{Coulomb}}. \quad (2)$$

Here $V = \pi R_{\text{out}}^2 R_e$ is the *effective available volume*, m_i (\vec{v}_i) is the mass (velocity) of particle i , and \vec{F}_{ij} (\vec{r}_{ij}) the force (connection vector) between particles i and j . The last term represents the Coulomb contribution to the pressure tensor and is calculated according to Ref. [52]. The side contribution P_{side} is obtained directly by measuring the average normal force on the constraint and dividing by its area. Having expressions for P_{cap} , P_{side} and P_{res} , we determine the equilibrium volume using $P_{\text{in}}(V_{\text{eq}}) = P_{\text{res}}$. To check the accuracy of the single-chain cell model we compare our equilibrium chain extensions to the ones obtained via the periodic-cell model, cf. Fig. 2 of Ref. [31]. We will discuss the results after describing the second mean-field approximation.

Since the single-chain cell model uses a cylindrical cell a further reduction of the model complexity is to construct an adapted PB description of the polyelectrolyte in the salt solution. As before, the PB model uses a semi-infinite cylinder having an external radius R_{out} and conceptual length R_e , as shown in Fig. 1. The electrostatics for an infinite rod is solved, again mimicking in a simplified way the electrostatic situation in a gel. We also depict how the explicit single chain is now modeled as a penetrable concentric charged rod of radius a , characterized by a prescribed charge distribution.

The radius a of the charged rod is chosen such that the polymer density implies the same average distance from the end-to-end vector as obtained from single-chain MD simulations. This amounts to finding the length scale equivalent to the tensional blob size. The numerical value is obtained via fitting a second degree polynomial $a_{\text{MD}}(R_e) = N\sigma (C_1(R_e/(N\sigma))^2 + C_2(R_e/(N\sigma)) + C_3)$, with $C_1 = -0.17$, $C_2 = 0.14$, $C_3 = 0.03$ based on our single-chain MD data. Enforcing $\langle r \rangle = \int_V p(\vec{r}) r dV \stackrel{!}{=} a_{\text{MD}}$ we obtain for the rectangular distribution function $a = 3/2 a_{\text{MD}}$. The monomer charges thus have a probability density $p(\vec{r}) = \mathcal{N} H(-(r-a))$, where $H(x)$ is the Heaviside function and \mathcal{N} a normalization such that $p(\vec{r})$ is a probability density. For a strong polyelectrolyte, the charge is homogeneously distributed in the rod with $\rho_f(\vec{r}) = -Nf e_0 p(\vec{r})$.

The Poisson equation describes the electrostatic interaction and ionic distribution in the system:

$$\nabla^2 \psi = -\frac{1}{\epsilon_0 \epsilon_r} \left(\sum_i q_i c_i(\vec{r}) + \rho_f(\vec{r}) \right). \quad (3)$$

The number densities of the ions c_i are related to the charge densities via $\rho_i(\vec{r}) = q_i c_i(\vec{r})$ given by standard PB theory (with the bulk potential $\psi^{\text{b}} = 0$):

$$c_i(r) = c_i^{\text{b}} \exp\left(-\frac{q_i \psi(r)}{k_B T}\right). \quad (4)$$

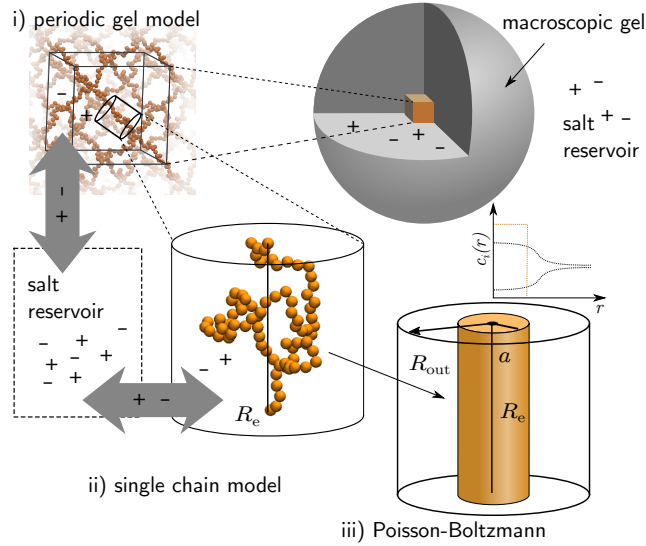


Figure 1: (Color online) A schematic of the i) macroscopic gel; ii) single-chain; and iii) PB model of a macroscopic gel in contact with a reservoir. The plot sketches a typical radial density profile.

Water is modeled implicitly via a relative dielectric permittivity of $\epsilon_r \approx 80$.

The PB pressure inside the cell P_{in} has two contributions: 1) The combined ideal and Maxwell pressure [53] which yields

$$P_{side} = k_B T c(R_{out}), \quad (5)$$

$$P_{cap}^{ions} = k_B T \langle c \rangle_z + \frac{\epsilon_0 \epsilon_r}{2} \langle E_r^2 \rangle_z, \quad (6)$$

where $E_r = -\partial_r \Psi(r)$ is the electric field in radial direction and $\langle \mathcal{A} \rangle_z = \int_0^{2\pi} \int_0^{R_{out}} r \mathcal{A}(r) dr / (\pi R_{out}^2)$ denotes the average over all radii. And 2) the stretching pressure P_{cap}^{str} (acting only on the cap) which we define to be the pressure due to confinement P^{conf} (in the spirit of [54, p. 115]) minus the tensile stress σ^{chain} of the chain in order to have a finite extension for a neutral polymer gel:

$$\begin{aligned} P_{cap}^{str}(R_e) &= P^{conf} - \sigma^{chain} \\ &= \frac{1}{\pi R_{out}^2} \left(\frac{k_B T}{b} \frac{R_0^3}{R_e^3} \mathcal{L}^{-1} \left(\frac{R_0}{R_{max}} \right) - \frac{k_B T}{b} \mathcal{L}^{-1} \left(\frac{R_e}{R_{max}} \right) \right), \end{aligned} \quad (7)$$

where \mathcal{L}^{-1} is the inverse Langevin function. The stretching pressure is constructed such that $P_{cap}^{str}(R_0) = 0$, where $R_0 = 1.2bN^{0.588}$ is the average end-to-end distance of an unconfined neutral chain [31]. For a neutral gel, only the stretching pressure will determine the swelling equilibrium $P_{in}(R_{eq}) = P_{res}$ which is found at $R_{eq} = R_0$. The added confinement pressure dominates at low extensions.

Therefore the pressure inside the gel can be obtained via Eq. (1) where the cap pressure is given by $P_{\text{cap}} = P_{\text{cap}}^{\text{ions}} + P_{\text{cap}}^{\text{str}}$. Applying the equilibrium condition $P_{\text{in}}(R_{\text{eq}}) = P_{\text{res}}$, we obtain the equilibrium end-to-end distance R_{eq} . All equations were solved with a finite element solver [55].

In the following, we compare the obtained swelling equilibria for both models to the periodic gel model for different charge fractions, chain lengths, and reservoir salt concentrations. For selected parameters, Fig. 2 demonstrates that for all models the gel swells: i) more with increased charge fraction f ; ii) less with higher salt concentration in the reservoir c_s^b , in good agreement with the data of the periodic gel model. Both models also work for Manning parameters larger than unity, contrary to the Katchalsky model [31]. Further, at high charge fractions ($f > 0.5$) they show better agreement with the periodic gel model than the self-consistent field theory presented in Ref. [32]. The PB model has basically the same accuracy as the single-chain MD model for the selected parameter regions. Enlarging the comparison across a wide parameter range to all available data, yielding 60 data points, Fig. 3 shows an excellent agreement of both models against the periodic gel model used here as the reference standard. Our PB model has the known limitations [56, 39]: multivalent ions, high charge densities (e.g. at high compressions of the gel) or high ionic concentrations lead to deviations due to neglecting ionic and excluded volume correlations which also exist in polyelectrolyte gels [57] or charged rod systems [39, 58]. However, these limitations do not apply to our single chain MD model.

We now generalize the PB model to account for weak groups similar to using the charge regulating boundary condition [59]. However, we use charge regulation as a way to determine the space charge density of the penetrable rod. For a weak polyelectrolyte where monomers may be neutral or charged ($\text{HA} \rightleftharpoons \text{A}^- + \text{H}^+$) the titratable monomers (A^- or HA) are distributed with $p(\vec{r})$ resulting in a concentration $c_0(\vec{r}) = Np(\vec{r})$. The dissociation constant is given by $K_a = c(\text{A}^-)c(\text{H}^+)/c(\text{HA}) = 10^{-4} \text{mol L}^{-1}$. Chemical equilibrium results in:

$$c(\text{A}^-, \vec{r}) = \frac{c_0(\vec{r})K_a}{c^b(\text{H}^+) \exp(-e_0\psi(\vec{r})/(k_B T)) + K_a}, \quad (8)$$

and therefore $\rho_f(\vec{r}) = -e_0c(\text{A}^-, \vec{r})$. In the case of charge regulation we also explicitly model pH (while neglecting any small OH^- concentration). Bulk charge neutrality implies that the sum of the product of all species multiplied with their valency needs to be zero (or equivalently):

$$c^b(\text{H}^+) + c^b(\text{Na}^+) = c^b(\text{Cl}^-) \quad (9)$$

Note that the bulk salt concentration c_{salt}^b is related to $c_{\text{Na}^+}^b = c_{\text{salt}}^b$ and $c_{\text{Cl}^-}^b = c_{\text{salt}}^b + c_{\text{H}^+}^b$ to ensure charge neutrality.

In Fig. 4, we show the equilibrium extension R_{eq} as a function of the $\text{p}K_a - \text{pH}$. The gel swells less with lower $\text{pH} = -\log_{10}(c^b(\text{H}^+)/(\text{mol/L}))$ ($\text{p}K_a - \text{pH}$ becoming larger) since the acid becomes less dissociated (less charged). The gel also swells less with higher salt concentration due to increased screening

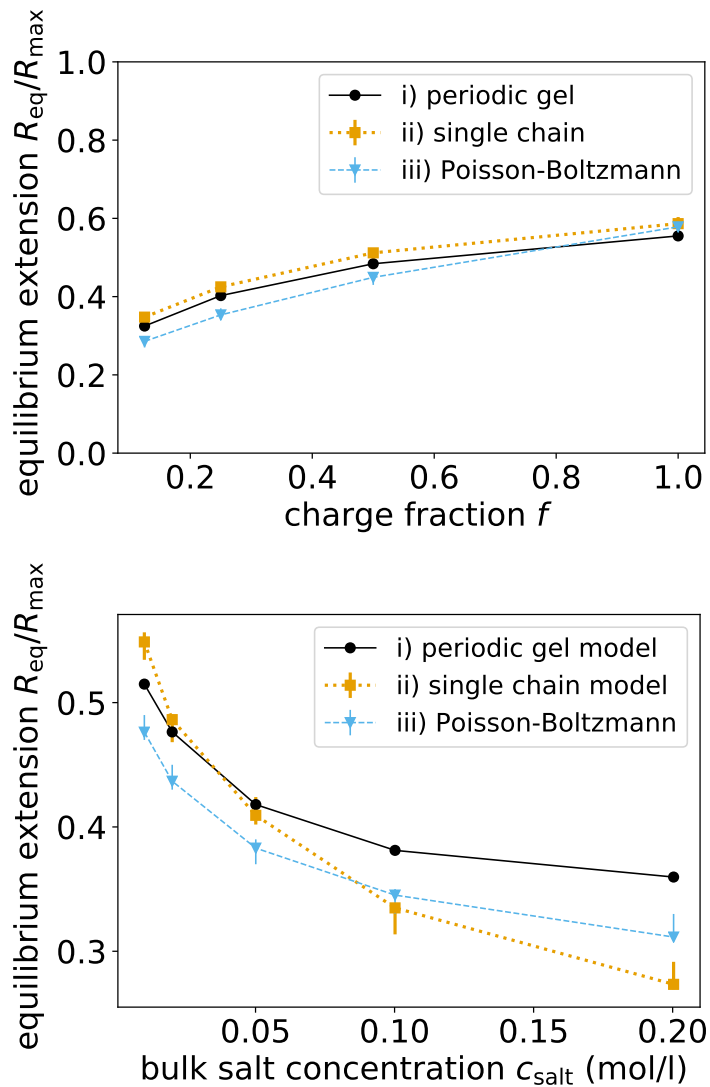


Figure 2: (Color online) Comparison between the three models. The equilibrium swelling length R_{eq} as a function of a) the charge fraction f along the gel polymer backbone for $c_{\text{salt}}^b = 0.01 \text{ mol L}^{-1}$ and $N \approx 80$; b) the salt bath concentration c_{salt}^b for $f = 0.5$ and $N \approx 60$. As can be seen in Fig. 3 the quality of the predictions of the single-chain model and the PB model for other parameter combinations are also very good.

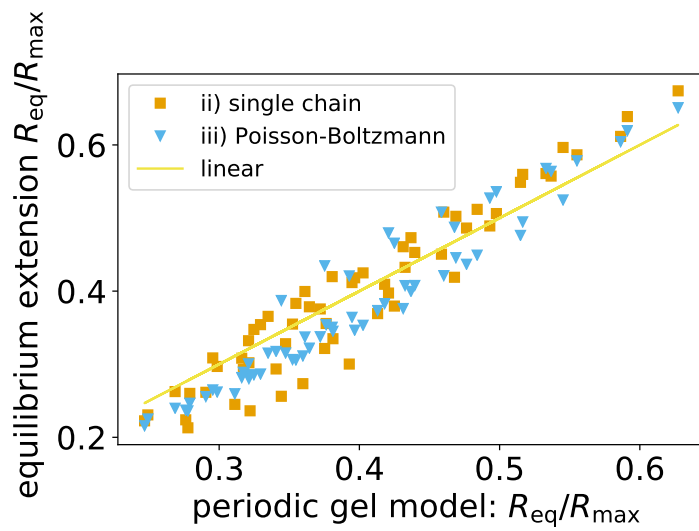


Figure 3: (Color online) The swelling equilibria of the single-chain cell model and the PB model compared to the periodic gel simulations. The results are compared for a wide exploration of in total 60 parameter combinations with $N \approx 40, 60, 80$, $f \in \{0.125, 0.25, 0.5, 1\}$ and $c_{\text{salt}}^b \in \{0.01, 0.02, 0.05, 0.1, 0.2\} \text{ mol L}^{-1}$. The linear function has the form $y(x) = x$.

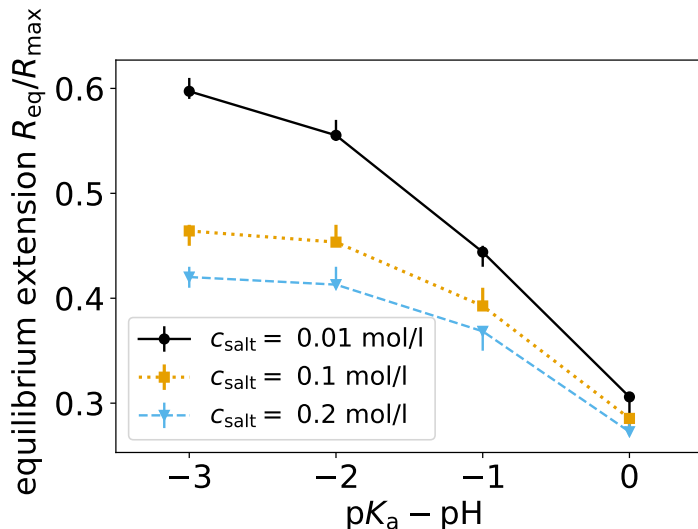


Figure 4: (Color online) The swelling equilibria as a function of $pK_a - pH$ for different salt concentrations $c_{\text{salt}}^b \in \{0.01, 0.1, 0.2\} \text{ mol L}^{-1}$ for $N = 59$ and $K_a = 10^{-4} \text{ mol L}^{-1}$.

and a higher pressure exerted by the salt reservoir. These findings are in good qualitative agreement with experiments [60, 61].

In summary, we presented two successively coarsening mean-field models that can predict swelling equilibria for charged macrogels. The first one, the single-chain cell model, is a charged bead-spring model with explicit salt ions confined within a cylindrical cell which can undergo affine volume changes. The computational cost for solving the single-chain cell model is at least an order of magnitude lower than for the periodic gel model. In the next model we replaced the charged single-chain and all ions by suitable charge distributions and use the PB framework to derive the equilibrium cylindrical cell length. This model can be solved numerically, i.e., with standard finite element solvers, and is yet at least another order of magnitude faster than the single-chain cell model. Since both models can predict the swelling equilibria in similar good agreement for a wide parameter range with the more elaborate periodic gel model, we can use the extremely efficient PB model for predictions about gel swelling equilibria. The PB model was further generalized to account for charged gels containing weak groups. We find that the gel behavior under different $pK_a - pH$ conditions as well as salt reservoir concentrations qualitatively agrees with experimental findings and theoretical expectations.

1 Acknowledgments

The authors acknowledge inspiring discussions with T. Richter and want to thank G. Rempfer and F. Weik for fruitful discussions regarding the pressure. Funding from the DFG through the SFB 716 and Grants HO 1108/26-1 and AR 593/7-1 is gratefully acknowledged.

References

- [1] Toyochi Tanaka, David Fillmore, Shao-Tang Sun, Izumi Nishio, Gerald Swislow, and Arati Shah. Phase transition in ionic gels. *Physical Review Letters*, 45(20):1636–1639, 1980.
- [2] *Polyelectrolyte gels: Properties, Preparation, and Applications*. ACS Symposium Series No. 480. American Chemical Society, Washington D.C., 1992.
- [3] N. A. Peppas, P. Bures, W. Leobandung, and H. Ichikawa. Hydrogels in pharmaceutical formulations. *European journal of pharmaceutics and biopharmaceutics*, 50(1):27–46, 2000.
- [4] X. Jia and K. L. Kiick. Hybrid multicomponent hydrogels for tissue engineering. *Macromolecular Bioscience*, 9:140–156, 2009.
- [5] J. Jagur-Grodzinski. Polymeric gels and hydrogels for biomedical and pharmaceutical applications. *Polymers for Advanced Technologies*, 21:27–47, 2009.
- [6] M. J. Zohuriaan-Mehr, H. Omidian, S. Doroudiani, and K. Kabiri. Advances in non-hygienic applications of superabsorbent hydrogel materials. *Journal of Materials Science*, 45(21):5711–5735, November 2010.
- [7] KS Kazanskii and SA Dubrovskii. Chemistry and physics of agricultural hydrogels. In *Polyelectrolytes Hydrogels Chromatographic Materials. Advances in Polymer Science*, volume 104, pages 97–133. Springer Verlag, 1992.
- [8] Johannes Höpfner, Tobias Richter, Peter Košovan, Christian Holm, and Manfred Wilhelm. Seawater desalination via hydrogels: Practical realisation and first coarse grained simulations. In Gabriele Sadowski and Walter Richtering, editors, *Intelligent Hydrogels*, volume 140 of *Progress in Colloid and Polymer Science*, pages 247–263. Springer International Publishing, 2013.
- [9] Tobias Richter, Jonas Landsgesell, Peter Košovan, and Christian Holm. On the efficiency of a hydrogel-based desalination cycle. *Desalination*, 414:28–34, 2017.
- [10] P. J. Flory and J. Rehner. Statistical mechanics of crosslinked polymer networks i. rubberlike elasticity. *Journal of Chemical Physics*, 11:512, 1943.

- [11] A. Katchalsky and I. Michaeli. Polyelectrolyte gels in salt solutions. *Journal of Polymer Science*, 15:69, 1955.
- [12] A. R. Khokhlov, S. G. Starodubtzev, and V. V. Vasilevskaya. Responsive gels: Volume transitions I. In K. Dušek, editor, *Conformational transitions in polymer gels: theory and experiment*, volume 109 of *Adv. Polym. Sci.*, page 123. Springer Verlag, New York, 1993.
- [13] M. Rubinstein, R. H. Colby, A. V. Dobrynin, and J. F. Joanny. Elastic modulus and equilibrium swelling of polyelectrolyte gels. *Macromolecules*, 29(1):398–406, 1996.
- [14] Gil C. Claudio, Kurt Kremer, and Christian Holm. Comparison of a hydrogel model to the poisson-boltzmann cell model. *The Journal of Chemical Physics*, 131(9):094903, September 2009.
- [15] Gabriel S. Longo, Monica Olvera de la Cruz, and I. Szleifer. Molecular theory of weak polyelectrolyte gels: The role of pH and salt concentration. *Macromolecules*, 44:147–158, 2011.
- [16] Manuel Quesada-Pérez, Jose Alberto Maroto-Centeno, Jacqueline Forcada, and Roque Hidalgo-Alvarez. Gel swelling theories: the classical formalism and recent approaches. *Soft Matter*, 7:10536–10547, 2011.
- [17] Prateek K. Jha, Jos W. Zwanikken, Juan J. de Pablo, and Monica Olvera de la Cruz. Electrostatic control of nanoscale phase behavior of polyelectrolyte networks. *Current Opinion in Solid State and Materials Science*, 15(6):271 – 276, 2011. Functional Gels and Membranes.
- [18] Andrea J Liu, Gary S Grest, M Cristina Marchetti, Gregory M Grason, Mark O Robbins, Glenn H Fredrickson, Michael Rubinstein, and Monica Olvera de la Cruz. Opportunities in theoretical and computational polymeric materials and soft matter. *Soft Matter*, 11(12):2326–2332, 2015.
- [19] Florian Müller-Plathe and Wilfred F. van Gunsteren. Solvation of poly(vinyl alcohol) in water, ethanol and an equimolar water-ethanol mixture: structure and dynamics studied by molecular dynamics simulation. *Polymer*, 38(9):2259 – 2268, 1997.
- [20] Thorsten Tönsing and Christian Oldiges. Molecular dynamic simulation study on structure of water in crosslinked poly(-isopropylacrylamide) hydrogels. *Physical Chemistry Chemical Physics*, 3:5542–5549, 2001.
- [21] Jonathan Walter, Viktor Ermatchkov, Jadran Vrabec, and Hans Hasse. Molecular dynamics and experimental study of conformation change of poly(n-isopropylacrylamide) hydrogels in water. *Fluid Phase Equilibria*, 296(2):164 – 172, 2010. VIII Ibero-American Conference on Phase Equilibria and Fluid Properties for Process Design.

- [22] Peter Košovan, Tobias Richter, and Christian Holm. Molecular simulations of hydrogels. In Gabriele Sadowski and Walter Richtering, editors, *Intelligent Hydrogels*, volume 140 of *Progress in Colloid and Polymer Science*, pages 205–221. Springer International Publishing, 2013.
- [23] Stefanie Schneider and Per Linse. Swelling of cross-linked polyelectrolyte gels. *The European Physical Journal E*, 8:457–460, 2002.
- [24] Quiliang Yan and Juan J. de Pablo. Monte carlo simulation of a coarse-grained model of polyelectrolyte networks. *Physical Review Letters*, 91(1):018301, July 2003.
- [25] Samuel Edgecombe, Stefanie Schneider, and Per Linse. Monte carlo simulations of defect-free cross-linked gels in the presence of salt. *Macromolecules*, 37(26):10089–10100, 2004.
- [26] De-Wei Yin, Qiliang Yan, and Juan J. de Pablo. Molecular dynamics simulation of discontinuous volume phase transitions in highly-charged crosslinked polyelectrolyte networks with explicit counterions in good solvent. *The Journal of Chemical Physics*, 123(17):174909, 2005.
- [27] Bernward A. Mann, Christian Holm, and Kurt Kremer. Swelling of polyelectrolyte networks. *Journal of Chemical Physics*, 122(15):154903, 2005.
- [28] Bernward A. Mann, Christian Holm, and Kurt Kremer. The swelling behaviour of charged hydrogels. *Macromolecular Symposia*, 237:90–107, 2006.
- [29] De-Wei Yin, Ferenc Horkay, Jack F. Douglas, and Juan J. de Pablo. Molecular simulation of the swelling of polyelectrolyte gels by monovalent and divalent counterions. *Journal of Chemical Physics*, 129(15), October 2008.
- [30] Manuel Quesada-Pérez, Jose Guadalupe Ibarra-Armenta, and Alberto Martín-Molina. Computer simulations of thermo-shrinking polyelectrolyte gels. *The Journal of Chemical Physics*, 135(9):094109, 2011.
- [31] Peter Košovan, Tobias Richter, and Christian Holm. Modeling of polyelectrolyte gels in equilibrium with salt solutions. *Macromolecules*, 48(20):7698–7708, 2015.
- [32] Oleg Rud, Tobias Richter, Oleg Borisov, Christian Holm, and Peter Košovan. A self-consistent mean-field model for polyelectrolyte gels. *Soft Matter*, 13(18):3264–3274, 2017.
- [33] Bernward A. Mann. *The Swelling Behaviour of Polyelectrolyte Networks*. PhD thesis, Johannes Gutenberg-University, Mainz, Germany, December 2005.
- [34] G. S. Manning. Limiting laws and counterion condensation in polyelectrolyte solutions I. colligative properties. *The Journal of Chemical Physics*, 51:924–933, 1969.

- [35] Markus Deserno and Christian Holm. Cell-model and poisson-boltzmann-theory: A brief introduction. In C. Holm, P. Kékicheff, and R. Podgornik, editors, *Electrostatic Effects in Soft Matter and Biophysics*, volume 46 of *NATO Science Series II - Mathematics, Physics and Chemistry*, pages 27–50. Kluwer Academic Publishers, Dordrecht, NL, December 2001.
- [36] T. Alfrey, P. W. Berg, and H. J. Morawetz. The counterion distribution in solutions of rod-shaped polyelectrolyteS. *Journal of Polymer Science*, 7:543, 1951.
- [37] R. M. Fuoss, A. Katchalsky, and S. Lifson. The potential of an infinite rod-like molecule and the distribution of the counter ions. *Proceedings of the National Academy of Sciences of the United States of America*, 37:579–589, 1951.
- [38] A. Katchalsky, S. Lifson, and J. Mazur. The electrostatic free energy of polyelectrolyte solutions. i. randomly kinked macromolecules. *Journal of Polymer Science*, 11(5):409–423, 1953.
- [39] Markus Deserno, Christian Holm, and Sylvio May. Fraction of condensed counterions around a charged rod: Comparison of Poisson-Boltzmann theory and computer simulations. *Macromolecules*, 33:199–206, 2000.
- [40] A. Deshkovski, S. Obukhov, and M. Rubinstein. Counterion phase transitions in dilute polyelectrolyte solutions. *Physical Review Letters*, 86(11):2341–2344, 2001.
- [41] Dmytro Antypov and Christian Holm. Optimal cell approach to osmotic properties of finite stiff-chain polyelectrolytes. *Physical Review Letters*, 96:088302, 2006.
- [42] Sergei Panyukov and Yitzhak Rabin. Statistical physics of polymer gels. *Physics Reports*, 269(1–2):1–131, 1996.
- [43] Hans Jörg Limbach, Axel Arnold, B. A. Mann, and Christian Holm. ESPResSo – an extensible simulation package for research on soft matter systems. *Computer Physics Communications*, 174(9):704–727, May 2006.
- [44] Florian Weik, Rudolf Weeber, Kai Szuttor, Konrad Breitsprecher, Joost de Graaf, Michael Kuron, Jonas Landsgesell, Henri Menke, David Sean, and Christian Holm. ESPResSo 4.0 – an extensible software package for simulating soft matter systems. *The European Physical Journal Special Topics*, 227(14):1789–1816, 2019.
- [45] J. D. Weeks, D. Chandler, and H. C. Andersen. Role of repulsive forces in determining the equilibrium structure of simple liquids. *The Journal of Chemical Physics*, 54:5237, 1971.

- [46] Gary W. Slater, Christian Holm, Mykyta V. Chubynsky, Hendrick W. de Haan, Antoine Dube, Kai Grass, Owen A. Hickey, Christine Kingsbury, David Sean, Tyler N. Shendruk, and Lixin Zhan. Modeling the separation of macromolecules: A review of current computer simulation methods. *Electrophoresis*, 30(5):792–818, 2009.
- [47] Gary S. Grest and Kurt Kremer. Molecular dynamics simulation for polymers in the presence of a heat bath. *Physical Review A*, 33(5):3628–31, 1986.
- [48] Daan Frenkel and Berend Smit. *Understanding molecular simulation*. Academic Press, San Diego, 2 edition, 2002.
- [49] Markus Deserno and Christian Holm. How to mesh up Ewald sums. I. A theoretical and numerical comparison of various particle mesh routines. *Journal of Chemical Physics*, 109:7678, 1998.
- [50] Markus Deserno and Christian Holm. How to mesh up Ewald sums. II. An accurate error estimate for the Particle-Particle-Particle-Mesh algorithm. *Journal of Chemical Physics*, 109:7694, 1998.
- [51] Dmytro Antypov and Christian Holm. The osmotic behavior of short stiff polyelectrolytes. *Macromolecular Symposia*, pages 297–306, 2006.
- [52] U. Essmann, L. Perera, M. L. Berkowitz, T. Darden, H. Lee, and L. Pedersen. A smooth Particle Mesh Ewald method. *Journal of Chemical Physics*, 103:8577, 1995.
- [53] Emmanuel Trizac and J.-P Hansen. Wigner-seitz model of charged lamellar colloidal dispersions. *Physical Review E*, 56:3137, 1997.
- [54] Michael Rubinstein and Ralph H. Colby. *Polymer Physics*. Oxford University Press, Oxford, UK, 2003.
- [55] COMSOL Multiphysics. *COMSOL Multiphysics User’s Guide*, 2012.
- [56] David Andelman. *Handbook of Biological Physics*, chapter 12, page 603. School of Physics and Astronomy, Tel Aviv University, 1995.
- [57] De-Wei Yin, Monica Olvera de la Cruz, and Juan J. de Pablo. Swelling and collapse of polyelectrolyte gels in equilibrium with monovalent and divalent electrolyte solutions. *Journal of Chemical Physics*, 131(19):194907–6, November 2009.
- [58] Markus Deserno, Felipe Jiménez-Ángeles, Christian Holm, and Marcelo Lozada-Cassou. Overcharging of DNA in the presence of salt: Theory and simulation. *The Journal of Physical Chemistry B*, 105(44):10983–10991, October 2001.

- [59] Barry W. Ninham and V. Adrian Parsegian. Electrostatic potential between surfaces bearing ionizable groups in ionic equilibrium with physiologic saline solution. *Journal of Theoretical Biology*, 31(3):405–428, June 1971.
- [60] Aharon Katchalsky. Rapid swelling and deswelling of reversible gels of polymeric acids by ionization. *Cellular and Molecular Life Sciences*, 5(8):319–320, 1949.
- [61] Toyochi Tanaka. Gels. *Scientific American*, 244(1):124–S, 1981.